

STRONG ENRICHMENT IN COPPER IN THE KIMBERLEY AREA, GALE CRATER, MARS. W. Goetz¹, V. Payre², R. C. Wiens³, O. Gasnault⁴, R. Gellert⁵, H. Newsom⁶, C. Fabre², O. Forni⁴, J. Lasue⁴, P.-Y. Meslin⁴, S. Maurice⁴, J. Frydenvang^{3,7}, M. B. Madsen⁷, B. Clark⁸, and the MSL Team, ¹Max Planck Institute for Solar System Research, Justus-von-Liebig-Weg 3, 37077 Göttingen, Germany (goetz@mps.mpg.de), ²Univ. of Lorraine, Nancy, France; ³LANL, Los Alamos, USA; ⁴IRAP, Univ. Toulouse, France; ⁵Univ. Guelph, ON, N1G 2W1, Canada; ⁶Univ. New Mexico, Albuquerque, USA; ⁷NBI, Univ. Copenhagen, Denmark; ⁸SSI, Boulder, CO, USA.

Introduction: The Curiosity rover has been exploring Gale crater, Mars, since Aug. 2012. Along her traverse the ChemCam and APXS instruments that are based on LIBS (Laser Induced Breakdown Spectroscopy) and X-ray fluorescence, respectively, have been used to track the chemical composition of rocks and soils near the rover [1, 2, 3, 4]. Both instruments are able to measure copper (Cu) abundances above ~50 ppm (ChemCam) and ~20 ppm (APXS) and indicate a background Cu level of <50 ppm. However, direct quantitative comparison of ChemCam to APXS data requires some modelling due to very different target foot prints & analytical depth: ~0.4 mm/sub- μ m per shot [5] (ChemCam) and ~16 mm/50 μ m (in the case of Cu) (APXS). A companion abstract [6] describes quantification of Cu (as based on ChemCam) along the rover traverse. Here we highlight soils and outcrops strongly enriched in Cu (>10 times above background!) in the Kimberley area by integrating ChemCam, APXS, and image/textural data.

Geochemical Significance of Copper: The average abundance of Cu in the terrestrial crust and mantle is estimated at 25 ± 10 ppm Cu [7,8]: by far the majority of crustal Cu is found as trace element in magmatic rocks (~100 ppm and ~10 ppm, respectively, in mafic and felsic rocks [9]), hosted by pyroxenes, plagioclases, olivine (typically ~100 ppm in the pure mineral phase [10]), or titanomagnetite [11]. A minor part of crustal Cu occurs in (potentially mined) sulfide ore deposits that typically form by separation of immiscible sulfides from upwelling magma or by precipitation from hydrothermal fluids/brines.

Copper enriched targets: Fig.1 shows the spectral range of ChemCam spectra that is diagnostic of Cu. Both Cu lines (324.85 and 327.5 nm) interfere significantly with Ti lines. The former appears as one broad “Cu-Ti” peak whose symmetry changes continuously as the Ti/Cu ratio decreases (fig. 1 a-c). The latter Cu line (mostly used for quantification [6]) is less perturbed by Ti so that targets with ordinary abundance of Ti and “sufficiently enriched” in Cu do show a partially resolved double peak in the region 327.2-327.5 nm. Table 1 provides Cu estimates [6] and Figures 2-4 show the geologic context of strongly Cu-enriched targets in the Kimberley area (including those highlighted in Fig.1). In some cases those targets (or targets close-by) were also studied by APXS although direct com-

parison is difficult (see above). There is no obvious textural or morphological feature indicative of Cu enrichment. Targets in Table 1 appear to be sedimentary outcrops (sandstones) except CC_BT_604a, Stephen, and Stirling_2 that are, respectively, a soil sample, a resistant fin, and a partially eroded surface feature (possibly of diagenetic origin). The soil sample is heterogeneous (also in terms of Cu abundances, Table 1). Mobile surface dust (characterized by the first few shots) is not carrying the high Cu signal. This is consistent with CC_BT_0604a (Fig.2a) whose high-Cu signal shows only up in the later shots (post #10).

| target | Cu [ppm] (ChemCam) | | Cu [ppm] (APXS) |
|-------------|---------------------|--------------|-----------------|
| | mean +/- 1 σ | max. (pt. #) | |
| Liga | 430 +/- 320 | 1050 (#5) | ~600 |
| Harms | 146 +/- 117 | 295 (#3) | - |
| CC_BT_604a | 115 +/- 187 | 868 (#6) | - |
| Stephen_DP | 111 +/- 24 | 131 (#1) | 200-350 |
| Stirling_2 | 142 +/- 161 | 563 (#9) | < 50 |
| Hayden_Peak | 271 +/- 166 | 699 (#1) | - |

Table 1: Cu abundances [ppm] of Cu enriched targets in the Kimberley area. The target names refer to ChemCam targets. APXS abundances refer to APXS data acquired on the ChemCam target such that in most cases the sample volume as probed by APXS included the one probed by ChemCam. ChemCam abundances computed by V. Payre.

Stephen rock (Fig.4) has a peculiar triangular shape and was studied extensively during the Kimberley campaign (sols 580-630). On sol 611 a ChemCam 3x3 raster experiment provided first information on chemical composition (e.g. high manganese [12]) and swept off the dust for later experiments. As a result the bluish shiny surface (Fig. 4) of Stephen was exposed. On sol 620 the “Stephen_DP” experiment showed decreasing Cu signal during the first 40 or 50 shots, followed by continuous slow decrease over the remaining shots (Fig.4). APXS measured high Cu abundance (> 200 ppm) in this target, but ChemCam tells us that this could be a surface feature. Contrary to Cu, the Zn abundance appears to be highest around shot ~60 (~20 μ m depth? [5]).

Conclusions and Discussion: We have described a soil and outcrops in the Kimberley area (sol 580-630), whose Cu-abundances exceed background level (~30

ppm) by a factor of >10 . The processes leading to this significant Cu enrichment are unknown. Cu's associations with other elements (e.g. Zn, Mn) must be further explored so that Cu can become a geochemical tracer for (ancient) chemical processes or a proxy for certain mineral assemblages on the surface of Mars.

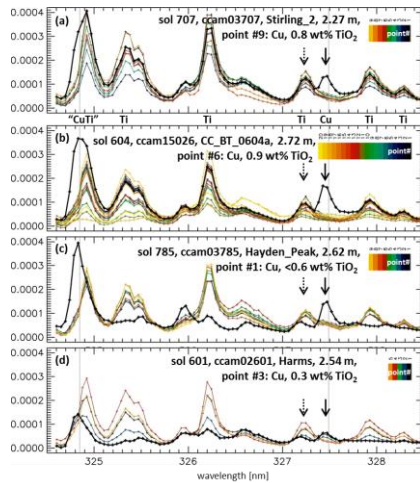


Fig.1: ChemCam shot-averaged and normalized spectra of Cu-bearing targets: (a) Stirling_2, (b) CC_BT_0604a, (c) Hayden_Peak, and (d) Harms, studied with 9, 20, 9, and 5 points, respectively (see colorbars). The spectrum of the Cu-rich point is drawn by a thick black line. Peak symmetry at ~ 324.8 nm changes continuously as the Ti/Cu ratio (solid black arrows) decreases from panel (a) through (c). Spectrum (d) displays presence of Cu near detection limit.

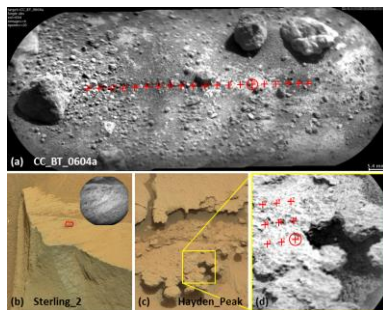


Fig.2: Geologic context for targets (a) CC_BT_0604a (red crosses are LIBS points, Cu-enriched point encircled), (b) Sterling_2 (LIBS points within red ~ 6 mm wide rectangle, inset is the 4.5 mm wide RMI view), and (c-d) Hayden_Peak with LIBS points as in (a). Images: (a) ChemCam-RMI, sol 604. Right Mastcam: (b) mcam03003, sol 707, (c) mcam03418, sol 785. (b, d) ChemCam-RMI images are from sol 707 & 785. Credit: NASA/JPL/MSSS/CNES/LANL.

Acknowledgements: This work is supported by CNES and the NASA Mars Program Office. WG received funding from DFG (GO 2288/1-1). Discussion with B. Lehmann, Univ. Clausthal, on copper is gratefully acknowledged.

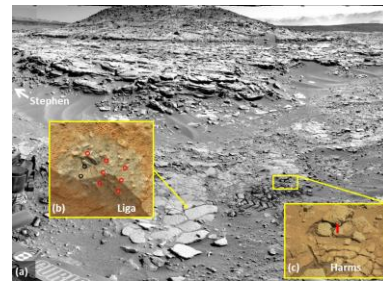


Fig.3: Geologic context for Harms (zoom in (c) in the Kimberley area. Its LIBS spectrum (Fig. 1d) was acquired along the vertical (~ 20 mm long) red line). Harms is part of play outcrop ahead of Mt. Remarkable, a meter-high butte in the background. Also highlighted: Target Liga (b), flat, partly shadowed outcrop, LIBS points within a circular previously cleaned area (~ 20 mm) and indicated by circles (red ones are enriched in Cu). Liga showed highest Cu signal ever as based on APXS (~ 600 ppm [13]) and ChemCam data [6]. Images: (a) Left Navcam, view towards WSW, sol 597, (b) MAHLI, sol 601, (c) Right Mastcam, mcam02534, sol 601. Credit: NASA/JPL/MSSS.

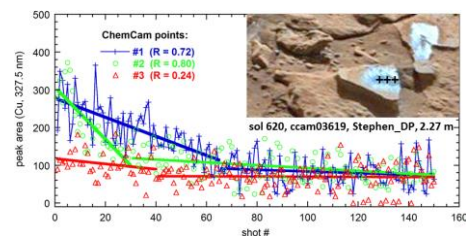


Fig.4: Dependence of Cu abundance (peak areas in rel. units) on depth for target "Stephen_DP" (located to the left of "Liga", right outside Navcam's field of view, Fig. 3a). Linear fits of early and later shots (with Pearson's R factors for fits of early shots) show that Cu is mainly at the surface. The inset shows the position of the ChemCam points (black crosses, 150 shots at each point). Image: Right Mastcam, mcam02659, sol 621. Credit: NASA/JPL/MSSS.

References: [1] Maurice, S. et al. (2012) Space Sci. Rev., 170, 95-166. [2] Wiens, R.C. et al. (2012) Space Sci. Rev., 170, 167-227. [3] Wiens, R.C. et al. (2013) Spectrochim. Acta B, 82, 1-27. [4] Campbell, J. L. et al. (2012) Space Sci. Rev., 170, 319-340. [5] Cousin, A. et al. (2011) LPSC, #1963. [6] Payré, V. et al. (2016) LPSC. [7] Rudnick RL, Gao S, 2003, Treatise on geochemistry, vol. 3: 1-64. [8] Lyubetska T. & Korenaga J (2007) J Geophys. Res. 112: B03211 [9] Pohl, W.L. (2011) Economic Geology, Wiley-Blackwell, UK, 5th ed., p.186. [10] Ure, A. & Berrow, M., 94-203, in: Bowen, H. J. M. (ed.) (1982) Environmental Chemistry, Royal Soc. Chem., London. [11] Alexander, P. O. & Thomas H. (2011) Bol. Inst. Fis. Geol., 79-81: 107-112. [12] N. Lanza, N. et al. (2014) AGU Fall Meeting, #P34A-05. [13] Gellert, R. et al. (2014) AGU Fall Meeting, #P34A-05.